Mechanism of low-threshold hypersonic cavitation stimulated by broadband laser pump

N. F. Bunkin,[1,*] A. V. Lobeyev,[1] G. A. Lyakhov,[1] and B. W. Ninham[2]
[1]*General Physics Institute of the Russian Academy of Sciences, Vavilova Street 38, 117942 Moscow, Russia*
[2]*Research School of Physical Sciences and Engineering, Department of Applied Mathematics, Australian National University, Canberra, Australian Capital Territory 2601, Australia*

(Received 20 May 1998; revised manuscript received 22 February 1999)

A low threshold acoustic cavitation regime was observed for the excitation of hypersonic waves due to a stimulated Brillouin scattering (SBS) mechanism, when the optical pump lies within the uv frequency range. Cavitation occurs if the optical pump bandwidth $\Delta_+ \gg \Omega_0$, where Ω_0 is the Stokes frequency shift (the hypersonic frequency). In the opposite case ($\Delta_+ \ll \Omega_0$), cavitation does not occur despite the fact that the hypersonic wave intensity is much higher. The effect is associated with the stimulation of a broad frequency spectrum of hypersonic pressure in a field provided by the broadband optical pump. In contrast, for a monochromatic optical pump, the hypersonic wave is of single-frequency character. Induction of cavitation at the low intensities of acoustic pressure is attributed to nanobubbles of fixed size that occur in the liquid. The resonant frequency of the nanobubbles coincides with the frequency of some spectral component of hypersound present in the broadband SBS process. That conclusion is reinforced by the further observation that at the same intensity of broadband pumping the cavitation vanishes after degassing the liquid. In parallel experiments on four-photon polarization Rayleigh wing spectroscopy, it was also demonstrated that spectral lines exist in ordinary (not degassed) water, which can be ascribed to resonances of radial vibrations of nanobubbles. Those lines are absent in the degassed water spectrum. [S1063-651X(99)06107-3]

PACS number(s): 47.55.Bx, 47.55.Dz, 42.62.Fi, 42.65.Es

I. INTRODUCTION

This work is concerned with the generation of intense hypersound for stimulating hypersonic cavitation. By hypersonic cavitation we mean here the formation of bubbles in a liquid caused by pressure, which changes with hypersonic frequency. Our interest in acoustic cavitation is associated with the well known fact, not yet explained, that the molecular strength of liquids (this is related primarily to water) is at least two to three orders of magnitude higher than the threshold for cavitation for ultrasonic frequencies [1]. (No experimental data on hypersonic cavitation have so far been available.) The discrepancy is usually explained by postulating the existence of vapor-gas bubbles of very small size in the liquid far from its boiling point. Such bubbles are assumed to be nuclei for cavitation, the presence of which facilitates rupture of a liquid by an acoustic pressure. This is the conventional ''explanation'' of acoustic cavitation. But it faces apparently insuperable difficulties.

According to extant theoretical notions, such bubbles can exist in diffusion equilibrium with the liquid only if their surface tensions are compensated in some unknown manner. Otherwise, the bubbles should collapse [2] due to huge compressive forces $\sim 2\alpha/R$ (α is the surface tension coefficient, R is the radius of the bubble). Thus the problem arises to invent some mechanism which might provide surface tension compensation. One possible mechanism advanced in [3] supposes that ions of the same sign may adsorb on the surface of a microbubble, giving rise to repulsive Coulomb forces over the surface (this is the so-called *ionic skin model*). For some critical value of the radius of bubbles, the negative electrostatic pressure could then compensate the compressive surface tension pressure, and a bubble may appear to be quasistable. Among the other models of surface tension compensation, it is worthy to mention the *rigid organic skin model* [4]; this model suggests that organic compounds could form a rigid skin about a surface of a free gas bubble and prevent it from dissolving. The organic skin was believed to be necessarily impermeable to gas diffusion and must have sufficient mechanical strength to overcome the hydrostatic and surface tension forces tending to collapse the bubble. However, this model was subsequently abandoned by the authors [5], because it apparently was inconsistent with the experimental study [6]. Another possible mechanism of the bubble stabilization is the *film of surface-active substances model*, which has been advanced in [7,8] and developed subsequently in [9,10]. This model is based on a supposition that detergents and soaps (which are present in liquids in trace amounts) tend to be composed of an oxygen-rich group on one end and a long hydrocarbon tail on the other. For an air bubble in water, the polar end will bond to the water surface and the tail will extend outward into the air. This ''picket-fence'' configuration has an intrinsic elasticity that may stabilize the microbubble. It is worthwhile to mention that the experimental results of the studies [7,8] were obtained for water containing near-saturation amounts of dissolved gas, while it has been found in [3] (the ionic skin model) that a change in the cavitation threshold with concentration of ionic solutes could not be detected until the amount of dissolved gas was reduced below approximately 45% of saturation. Thus, the evidence of works [7,8] does not at all rule out the ionic skin stabilization model [3]. Finally, one of the earliest models proposed for the bubble stabilization [11] suggests that gas is trapped in a conical crevice in a solid particle present in the liquid. This model has received considerable

*Author to whom correspondence should be addressed. Electronic address: nBunkin@kapella.gpi.Ru

attention and has been examined in [6,12–15], and assumes that a pocket of gas entrained in a crevice in a solid particle can exist steadily; this gas pocket is thought to be a nucleus not only for cavitation but also for boiling.

Note that all these models explain convincingly the presence of the cavitation effect in a wide frequency range of acoustic waves. Our specific interest is associated with an experimental study of hypersonic cavitation. Indeed, it is known that the cavitation strength of liquids increases steeply with the rising frequency of sound [1], and the question arises whether it is possible to induce the cavitation at the hypersonic frequencies. Indeed, let us estimate the size R of a bubble, which has the resonant frequency in the hypersonic range. This size is found from the formula [16]

$$f_{\mathrm{res}}=(1/2\pi R)\left[\frac{3\gamma}{\rho}\left(P+\frac{2\alpha}{R}\right)\right]^{1/2}, \tag{1}$$

where a liquid is characterized by density ρ, the hydrostatic pressure P, and the surface tension coefficient α, while γ is an adiabatic index. Requiring for the sake of argument $f_{\mathrm{res}}=10^{10}\,\mathrm{Hz}$ (which corresponds to hypersound), $P=1$ atm, and taking for water $\alpha=25\,\mathrm{erg/cm^2}$, we find $R=10\,\mathrm{nm}$. (Note that in our recent experiment on the low-angle neutron scattering from pure water [17], we have obtained evidence that there do exist spherical particles of size 4–5 nm in purified water of resistivity 18 $\mathrm{M\Omega\,cm}$.) We took in Eq. (1) a typical macroscopic value of the surface tension α; this is hardly justified because it is known that α reduces with a decreasing radius of a bubble, approaching zero in the limit of zero radius (see, for instance, [18]), i.e., we estimated R only qualitatively. It is also easy to find the bandwidth Δf of the resonant line of a bubble of such a small size (hereafter we will call these bubbles *nanobubbles*). The Noltingk-Neppiras equation [19], describing radial oscillations of a bubble, gives

$$\Delta f=(2/\pi)(\xi+4/3\eta)/\rho R^2. \tag{2}$$

Here ξ and η are coefficients of bulk and shear viscosity. Substituting $\xi\sim\eta=10^{-2}\,\mathrm{g/cm\,s}$, $R=10\,\mathrm{nm}$, we have for water $\Delta f\approx 1.5\times 10^{10}\,\mathrm{Hz}\sim f_{\mathrm{res}}$. It follows from here that the nanobubbles would probably not be high-quality oscillators, since the oscillation quality factor would be $Q=f_{\mathrm{res}}/\Delta f\sim 1$. Note that the amplitude of nanobubble oscillation lies in a nanometer region, in which, as for surface tension, the values of ξ and η are not known. [Yet again, the extensive experimental and theoretic data presented in the study [1] predict that it is possible to ignore the inertial reaction of liquid (actually its viscosity), if the bubble size is less than 10^{-3} cm.] Hence a theoretical estimate of Q can be at best within an order of magnitude. In what follows we present some experimental results which enable one to make more realistic conclusions on the existence of, and the bandwidth of, nanobubble oscillations.

By using the results of the studies [19,20], we can calculate the cavitation threshold for the nanobubbles of radius 10 nm; this pressure is ~100 atm. Thus to detect this cavitation one should have a powerful enough transducer for hypersonic waves, which poses a challenging problem to experimental physicists. In what follows we present experimental results which can be interpreted as an essential decrease of the cavitation threshold for hypersound. If it turns out to be so, it will call for some new models of the gas bubble dynamics in the nanoscale range. As will be clear from the following, our study is concerned with seeking resonant lines in water for hypersonic frequencies. The estimates above suggest that nanobubble resonant lines (for water) would fall into the microwave band of electromagnetic radiation, and there is no information on the existence of narrow resonant lines for water in the frequency range $\sim 10^{10}$ Hz. Water absorbs electromagnetic radiation strongly over an extensive frequency range, including the far ir and microwave frequencies. Any possible nanobubble resonant lines would be obscured by an intense background of the water absorption spectrum for microwave frequencies. Given that apparently insuperable obstacle, we have therefore applied another technique (specifically, the four-photon interaction scheme) for inducing the excitations of the medium in that frequency range. Here we describe an experiment, based on the four-photon polarization spectroscopy of water for the frequency range $0-2\ \mathrm{cm^{-1}}$, which corresponds to $(0-6)\times 10^{10}$ Hz. It is this frequency interval, according to the estimates above, which should contain resonant frequencies of nanobubbles of our interest.

The experiments were carried out for degassed and nondegassed water. The idea to compare these liquids is based on natural hints that degassed water is free of gas bubbles or, more realistically, their density in a degassed water should decrease as compared to nondegassed water. (Our special interest in the degassed water explorations was motivated by the studies of an optical breakdown of degassed and nondegassed water [21–23]; it follows from these works that the optical breakdown threshold rises steeply after degassing, which points to a certain similarity of the phenomena of optical breakdown and acoustic cavitation.) The experiment shows that there do indeed exist narrow spectral lines in this frequency range for water containing dissolved gas. We believe it to be an important and significant observation that these lines are absent for degassed water, a fact providing indirect evidence for the existence and nature of the nanobubbles (leaving aside the question of their stabilization mechanism). Subsequently, we describe another experiment in which we managed to stimulate hypersonic waves at the frequency of supposed nanobubble resonance, and detect low-threshold hypersonic cavitation. This reinforces the suggestion that the resonances observed in the four-photon polarization spectroscopy experiment can be ascribed to radial vibrations of bubbles of a nanometer scale.

II. EXPERIMENT

The idea behind polarization spectroscopy is well known. It lies in the fact that any dynamic molecular process contributes to fluctuations of local liquid anisotropy, thus depolarizing initially polarized radiation in a process of scattering. The light scattering by the anisotropy fluctuation is also termed Rayleigh wing scattering [24]; the Rayleigh wing line is centered at the zeroth frequency, and its spectral width is determined by an inverse time of the anisotropy relaxation. It is clear that the molecular periodic motions can contribute to

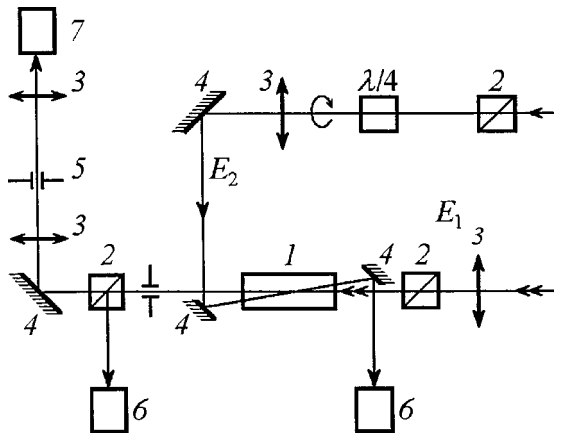

FIG. 1. Schematic of a setup for the four-photon polarization spectroscopy experiment. (1) The cell with a test liquid; (2) Glan prisms; (3) lenses; (4) mirrors; (5) spatial filter; (6),(7) photomultipliers.

local anisotropy, and the latter attains high magnitudes at resonances. This is why the Raman resonances can depolarize the light scattering as well (an extent of this depolarization depends on the symmetry properties of a particular resonance), and may be superimposed on the Rayleigh wing spectrum.

Application of the four-photon mixing technique to the polarization spectroscopy offers new possibilities for studying spectra by comparison with spontaneous spectroscopy. An opportunity is presented that considerably increases the signal-to-noise ratio, typically by a factor 10^2-10^3. This is due to the coherent phasing of molecular vibrations (and other dynamic processes) in a macroscopic volume, stimulated by a pair of interacting electromagnetic waves $E^{(1)}$ and $E^{(2)}$ at the frequency $(\omega_1-\omega_2)$, which is a common feature for all kinds of the coherent four-photon spectroscopy (see, for instance, [25]). We applied a degenerate scheme of interaction $\omega_2=\omega_1-(\omega_1-\omega_2)$; resonant excitations of the tunable frequency $(\omega_1-\omega_2)$ contribute to the overall depolarization, i.e., the behavior of the signal at the frequency ω_2 carries information on resonances in the frequency range $(\omega_1-\omega_2)$. The intensity of the depolarized radiation at frequency ω_2 is proportional to $\{|\chi^{(3)}_{ijkl}|E^{(1)}_j E^{(1)*}_k E^{(2)}_l\}^2$, where $\chi^{(3)}$ is the cubic susceptibility of medium, and $E^{(1)}_j, E^{(2)}_k$ are components of the vector of electrical field strength of interacting waves. Note that this technique has been successfully employed by us in our recent explorations of interior liquid structure [26].

The schematic of an experimental setup (actually only the part related to the four-photon mixing) is shown in Fig. 1. Experiments were carried out with a master laser, operated in a single longitudinal mode of bandwidth $\leqslant 0.05$ cm^{-1}, and three amplifiers on a YAG:Nd laser (the pulse duration is $\tau = 10$ ns and the total energy $E \cong 100$ mJ) and a C-500 dye-laser (Exciton, Inc.) with transverse pumping and a grazing-incidence diffraction grating (2400 grooves/mm), pumped by the third harmonic of a YAG:Nd^{3+} laser (all of these are not illustrated in Fig. 1). A 1200 grooves/mm diffraction grating, operating in the autocollimation regime in the second order of diffraction, was employed as a rear mirror of the dye laser. The dye-laser radiation was frequency tunable over a range 480–550 nm with a bandwidth $\leqslant 0.1$ cm^{-1}. This last naturally limited the apparatus line, i.e., the spectral resolution.

The beam of circularly polarized second harmonic of the master laser at frequency $\omega_1 = 19\times10^3$ cm^{-1} ($\lambda = 532$ nm) and the linearly polarized dye-laser beam at variable frequency ω_2 interact in the cell with liquid l (the planar polarization was implemented by the Glan prism 2, whereas the circular polarization was realized by a subsequent use of the Glan prism and the λ/4 plate). The beams propagate in nearly opposite directions and cross one another in the cell with liquid at an angle of about 2°. The legitimate signal was separated from the nonscattered dye-laser radiation by another Glan prism and a spatial filter 5. The nonscattered dye-laser radiation and the second-harmonic signal were detected by photomultipliers 6, while the scattered radiation was detected by photomultiplier 7. Then the signals passed to gated analog-to-digital converters. The computer simultaneously digitized energy of pulses from both lasers, normalized the legitimate signal energy to the dye-laser energy in each pulse, controlled the dye-laser frequency tuning, and performed the statistical processing of the recorded signals. Each experimental spectral point was taken with frequency step 0.2 cm^{-1}, and experimental error of these points was preset beforehand at 2%. This prescribed the necessary number of laser pulses at a given particular frequency of the dye laser. The level of the scattering signal was $10^{12}-10^{13}$ photons per pulse in the spectral maximum.

As was indicated earlier, our specific subject was degassed (which supposedly is free of nanobubbles) and nondegassed water. The degassing technique employed by us was adopted from the study [27]. Specifically, in our degassing apparatus 300 cm^3 of water could be degassed down to the base pressure of the pump (0.01 torr) in 1–2 h. The apparatus was made from a 1 liter suction conical (spreading toward the bottom) flask with two Teflon stopcocks, and magnetic stirring bar (the magnet was coated by a Teflon shell). Vigorous stirring splashed water up on the walls of the flask where the liquid ran down in a film for increasing its surface (this provided rapid degassing). The flask was coupled to the pump through a condenser supplied with circulating coolant (to minimize the loss of a liquid), a Teflon stopcock, and a liquid nitrogen trap (this unit served to measure the pressure of a ''dry'' gas, free of liquid vapor). The pressure inside the trap was controlled by a vacuum thermocouple gauge. The basic procedure was as follows. First the liquid nitrogen trap is evacuated. Then this section is closed off from the pump and opened briefly (about 5 sec) to the degassing apparatus. The pressure is read. The process is repeated until the pressure in the trap reaches the base pressure of the pump, and the subsequent repetitions of the procedure have no effect (this means that the content of residual gas is $\leqslant$1% of saturation). This normally takes 40 expansions. The degassed water was decanted away from the flask through the bottom Teflon stopcock directly to the experimental cell (the cell was evacuated beforehand). After filling the cell, the latter was hermetically sealed by another Teflon stopcock. Breaking the cell hermeticity and settling water in such an open state over 1–2 days allowed saturation with dissolved air: In this way nondegassed water was obtained. Note finally that the same cell was used for experiments on

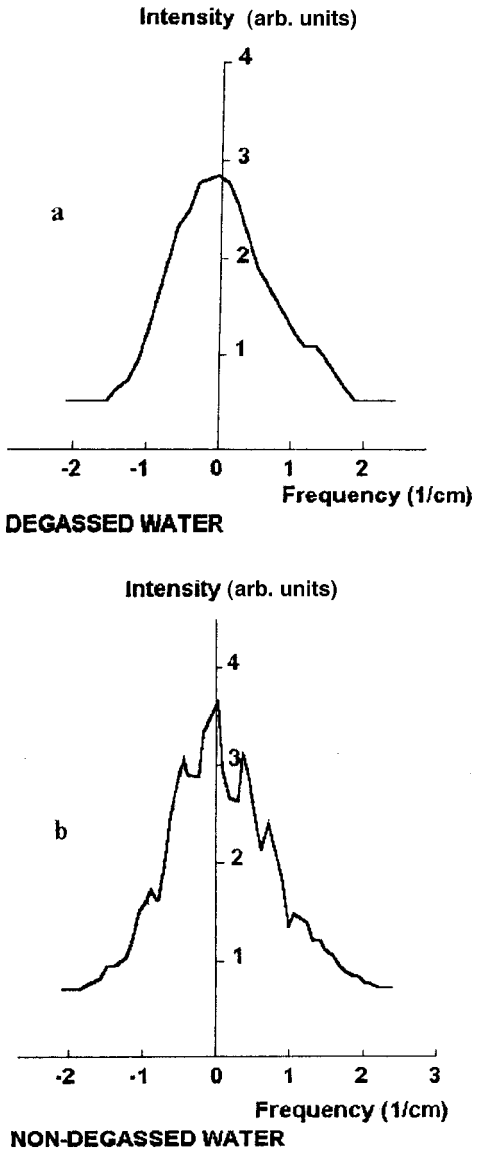

FIG. 2. Spectrum of water in the spectral range -2 to 2 cm^{-1}. (a) Degassed water; (b) nondegassed water.

the four-photon spectroscopy and the stimulated Brillouin scattering (SBS, see below).

In Fig. 2 we can see the spectra of degassed and nondegassed water (actually the intensity of the depolarized part of the dye-laser radiation), which are plotted versus the frequency difference $\Omega=\omega_1-\omega_2$ within the spectral range $\Omega=-2$ to 2 cm^{-1} (recall that ω_1 is the pump frequency and ω_2 is the tuned frequency of the dye-laser radiation). This range corresponds to the so-called narrow part of the Rayleigh wing, which is believed to have an origination from the rotational diffusion of molecules (see Ref. [24]). The experimental graphs were smoothed over nine succeeding points. We remark again here that the experimental error was preset beforehand and amounted to 2%. From Fig. 2(a) we can see that the spectrum of degassed water is free of any peculiarities. (Note here that the spontaneous Rayleigh wing spectroscopy [24] generally gives such a smooth spectral contour for all liquids under normal conditions.) The spectrum of the nondegassed water, which was subject to the same radiation characteristics, is shown in Fig. 2(b). It can be seen that this spectrum, as opposed to the case of degassed water, contains narrow peaks centered at 0.5 and 1 cm^{-1}. In our opinion, the observation of these peaks has been made possible by the use of the technique of very high sensitivity (see above). Note finally that the spectra of nondegassed water are very well reproducible; the reproducibility of degassed water spectra (for a given sample) is also quite satisfactory.

It is seen that the spectra in Fig. 2 are slightly asymmetric with respect to the zeroth frequency $\Omega=0$ (the latter was determined by the maximum of the measured signal). In our opinion, this asymmetry is due to certain nonlinear-optical effects revealed at the four-photon interaction (by contrast, in the spontaneous spectroscopy these effects do not show up, and the Rayleigh wing spectrum is symmetric about $\Omega=0$, see [24]). These effects are manifested in a different way at $\Omega<0$ and $\Omega>0$. Specifically, if the frequency ω_1 of an intense pump wave exceeds the probe wave frequency ω_2, i.e., $\Omega>0$, the energy transfer from the pump wave to the probe wave becomes possible; that is the so-called parametric amplification (see, for example, [25]). This effect is absent at $\omega_2>\omega_1$, which naturally explains the spectral asymmetry at $\Omega=0$. This should be taken into account at $G_{\mathrm{B,Ra,R}}I(\omega_2)l>1$ (the latter is valid for small Ω), where l is the interaction length of waves ω_2 and ω_2, while $G_{\mathrm{B,Ra,R}}$ is an increment of the SBS, the stimulated Rayleigh wing scattering (SRWS), and the stimulated Raman scattering (SRS), respectively. These processes provide the physical mechanisms for the parametric amplification, and we can expect the revelation of the parametric amplification due to SBS, SRWS, and SRS only at $\Omega>0$. Note that the Brillouin line is centered at 0.25 cm^{-1}, but it will hardly be pronounced in the spectra of degassed and nondegassed water. Indeed, by our calculations the bandwidth of this line is 6×10^{-3} cm^{-1}, whereas the tuning of the dye-laser frequency is made discretely by a step 0.2 cm^{-1}, and the spectral resolution of our setup is 0.1 cm^{-1}, i.e., the Brillouin line in all likelihood will not be detected (it can give a certain ''spike'' in the experimental graph profile, but this spike will be thrown away at the computer processing). At the same time, the spectral width of the narrow part of the Rayleigh wing is 1 cm^{-1}, and the SRWS can apparently contribute to the asymmetry. The same is true for the SRS, and the Raman lines are therefore more prominent at $\Omega>0$. We understand, however, that the question of spectral asymmetry due to the nonlinear-optical effects calls for special exploration, because it seems likely that these effects are manifested in a different way in degassed and nondegassed water.

To sum up so far, the experimental data obtained for both degassed and nondegassed water samples allow us to conclude that the effects of dissolved gas are revealed by the presence of narrow lines. These are superimposed on the Rayleigh wing line and centered at frequencies of 0.5 and 1 cm^{-1} (which corresponds to 1.5×10^{10} and 3×10^{10} Hz), i.e., they are of the same order as the resonant frequencies anticipated for nanobubble oscillations, see formula (1). Note too that a computer representation of the nondegassed water spectrum as a set of lines of Lorentzian shape, centered at 0, 0.5, and 1 cm^{-1}, enables one to make some judgment on the bandwidths of these lines. The bandwidth of the lines at 0, 5, and 1 cm^{-1} is about 0.2 cm^{-1}, i.e., 0.3×10^{10} Hz, which is a factor of 2 lower than the theoretical estimate of the band-

width for nanobubble resonance, see Eq. (2). This is hardly significant and would result from substituting the macroscopic values of bulk and shear viscosity into formula (2), while those values may be less in nanoscale.

As the bubbles in a liquid are usually assumed to be nuclei for acoustic cavitation, it is thus reasonable to study the cavitation at the tuning of the acoustic wave frequency within the range $0.5–1\,\mathrm{cm}^{-1} \Leftrightarrow (1.5–3)\times 10^{10}\,\mathrm{Hz}$, i.e., within the hypersonic band. The only means for generating hypersound in liquids is the SBS process [25,28]. Recall that this phenomenon is as follows: on reaching a definite intensity threshold, the powerful (pump) optical wave $E_p(\omega_p)$ is scattered by the density fluctuations of the medium, giving rise to an oppositely directed Stokes E_s (ω_s) wave and a copropagating hypersonic wave. The Stokes and the hypersonic waves gain energy from the pump wave and are so amplified. The mechanism which lies at the basis of SBS is just an electrostriction: the pump and the Stokes wave interaction shows up in a hypersonic pressure:

$$p(\Omega_0=\omega_p-\omega_s)=(1/8\pi)(\rho\partial\varepsilon/\partial\rho)E_p(\omega_p)E_s^*(\omega_s), \quad (3)$$

where Ω_0 is the hypersonic frequency. The Stokes and hypersonic waves should be simultaneous solutions of the equation for electrostriction and the Navier-Stokes equation [28]. It follows from here that the frequency of hypersound should satisfy the condition

$$\Omega_0=(2vn\omega_p/c), \quad (4)$$

where v and c are the velocities of hypersound and light, and n is the refractive index of the medium. In accordance with this expression, in order to obtain hypersound in the frequency range of interest to us [i.e., $\sim 10^{10}\,\mathrm{Hz}$, see Eq. (1)], the optical pump frequency ω_p should be about $10^{15}\,\mathrm{Hz}$. Thus the wavelength of the optical wave should be scanned within the range 200–400 nm (in the uv spectrum). Unfortunately, powerful laser sources with the possibility of scanning frequencies in that range are not available. This is the main challenge in conducting this experiment. Notwithstanding this obstacle, we did succeed in inducing hypersound within the required frequency range. This was accomplished by using broadband optical pumping. In what follows we describe an experiment for stimulating cavitation in a field of intense broadband uv radiation.

In this experiment we used an excimer Xe-Cl laser ($\lambda = 308\,\mathrm{nm}$, which corresponds to the frequency $\omega_p = 9.75\times 10^{14}\,\mathrm{Hz}$) and a pulse duration $\tau = 20\,\mathrm{ns}$, with a repetition frequency for laser pulses of 10 Hz. Substituting ω_p into Eq. (4), we find for water the hypersonic wave frequency of $\Omega_0 = 1.26\times 10^{10}\,\mathrm{Hz} = 0.42\,\mathrm{cm}^{-1}$. It follows from this that the frequency of the hypersonic wave, pumped by the radiation at 308 nm, belongs to the frequency range within which the resonant frequencies of nanobubbles supposedly lie (but do not necessarily coincide with those resonant frequencies). A schematic of an experimental setup is depicted in Fig. 3. We could implement a broadband or narrowband regime of generation of the Xe-Cl laser *l*. The broadband case of lasing had the following characteristics: the laser pulse energy W was up to 50 mJ and the bandwidth $\Delta_+ = 15\,\mathrm{cm}^{-1}$, i.e., it is substantially higher than the hypersonic frequency Ω_0. It was

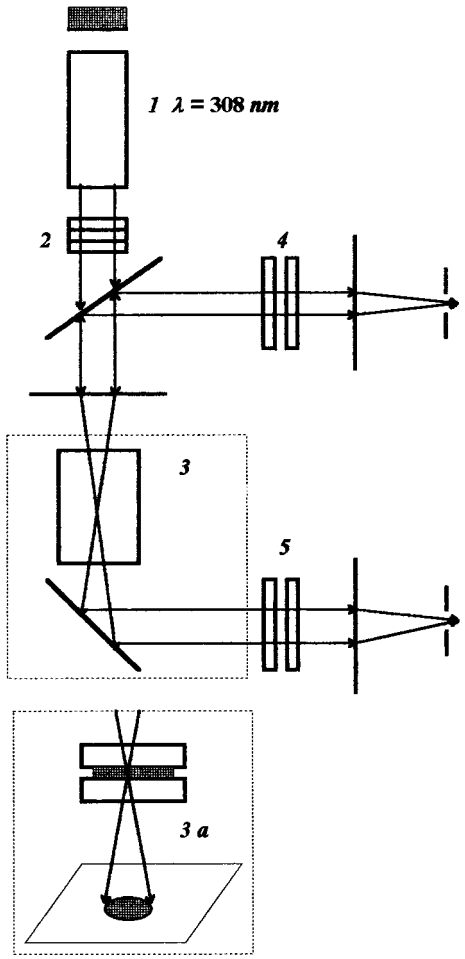

FIG. 3. Schematic of a setup for the cavitation experiment. (1) a Xe-Cl laser; (2) the optical stack; (3 or 3a) the cell with test liquid, having a longitudinal size 20 cm or 20 μm; (4,5) the Fabry-Perot interferometers.

possible to narrow the spectrum of pumping (more precisely, to rarefy it, with the aid of specially manufactured optical stack 2). We obtained two lines of bandwidth $<0.1\ \mathrm{cm}^{-1}$ with a frequency interval of $0.7\ \mathrm{cm}^{-1}$. The energy of the pulse of the narrow spectrum was enhanced by two amplifiers (they are not illustrated in Fig. 3), the final value of energy amounting to 10 mJ.

The test liquids were degassed and nondegassed water, hexane, and methyl alcohol. Our preliminary measurements have shown that the linear absorptivity at $\lambda = 308\,\mathrm{nm}$ is $\delta \sim 0.1\,\mathrm{cm}^{-1}$ (for water and methyl alcohol), and $0.06\ \mathrm{cm}^{-1}$ for hexane, i.e., any strong absorption resonances are apparently absent for this wavelength. Let us estimate the heating ΔT in the caustic at the broadband pump (the laser radiation underwent focusing; see below). By our measurements, the caustic radius was $r = 0.1\,\mathrm{mm}$. Ignoring the heat transfer effects (which evidently can only lower the heating), we have at $W = 50\,\mathrm{mJ}$ for water an estimate $\Delta T = \delta W/\rho\pi r^2 C_p = 25\,\mathrm{K}$, where ρ and C_p are the density and the heat capacity of water, respectively. Thus the linear absorption cannot result in boiling in the caustic.

With these preliminaries established, consider first the case of a broadband pumping. The laser pulse was directed

by a lens to the cell with the test liquid 3, having a longitudinal size 20 cm. On attaining some threshold intensity I_{thr}, the cavitation was observed as the tracks of tiny bubbles appearing along the waist of the laser beam. The bubbles floated up from the beam waist area and did not vanish during some time (more information about stability of the cavitation bubbles is below). Simultaneously, the beam cross section increased approximately by a factor of 5, evidently due to the scattering by the bubbles. The cavitation died out after a repeated ''shooting'' of some fixed area of nondegassed liquid within ~10 min (recall that the pulse repetition frequency was 10 Hz). This seems to be associated with the shooting area becoming depleted of bubbles—the cavitation nuclei. The cavitation resumed after some period of time without shooting. That time was necessary for a diffusion reenrichment of the shooting area with bubbles. Cavitation was renewed also on shifting the beam focus to another place inside liquid.

It is important to note that for the same value I_{thr}, a Stokes signal of intensity $I_- \sim 0.1 I_{thr}$ was detected. At the same time, while cavitation could not be induced in degassed water, the Stokes signal was nonetheless observed there for the same threshold intensity I_{thr}. The level of the Stokes wave was $I_- \sim (0.15-0.2) I_{thr}$, i.e., slightly higher than that for nondegassed water (this could be explained by destroying the pattern of interaction of light waves by cavitation bubbles, which leads to a decrease of the Stokes wave intensity).

The main experimental observation was as follows: at the same intensity of incident light I_{thr} (and even at an order of magnitude higher), the cavitation was absent for the laser pulses of a narrowed spectrum. This is additional evidence that the formation of bubbles for the broadband pump has nothing to do with linear absorption of laser energy. Indeed, the resonant line, if it exists, should absorb both the broadband and the narrowband radiation, whereas the effect ceased completely after narrowing the pump bandwidth, although in this case the light intensity was in excess of the broadband pump intensity. Besides, in the case of a narrowband pump, the intensity of the Stokes wave $I_- \sim (0.6-0.7) I_{thr}$, i.e., substantially higher than that for the broadband case for both degassed and nondegassed water. This can be explained by more effective interaction of light and hypersonic waves for the narrowband pump. Inasmuch as the stationary intensity of hypersound is $\mathcal{I} \sim I_- I_{thr}$ [25], it should be higher for the narrowband case. Thus we are faced with an apparent paradox: in the case of powerful hypersound we do not observe cavitation. In the case of weak hypersound we do observe the formation of bubbles. We remark parenthetically that for the broadband pumping we could not define the Stokes shift because the Stokes signal spectrum was of low intensity and had a blurred character. Fortunately, for the narrowband pump the spectrum of the Stokes wave as well as the Stokes shift value Ω_0 could be determined reliably by the Fabry-Perot interferometers 4.5. The measurements gave a value of $\Omega_0 = 0.2\ \mathrm{cm}^{-1}$, while the theoretic estimate gives $\Omega_0 = 0.42\ \mathrm{cm}^{-1}$ (see above). There is little need to analyze here the reasons for such a discrepancy, which seems to be a common feature for SBS by uv laser pumping (some model for explaining that discrepancy has been suggested in [29]).

We remark that the similar case of the formation of bubbles was also observed in another study [30] (the process there being termed ''boiling'') on the SBS in liquids using the broadband Xe-Cl laser pump. It was also noted in [30] that the cavitation disappears after narrowing the spectrum of a pump despite a substantial increase in its intensity. That phenomenon was explained in [30] by the fact that in a case of a narrowband pump, the Stokes wave is very efficiently generated over the full length of the beam path in the liquid. Therefore, the intensity of a pump may be depleted strongly prior to the focal region. In the opinion of the authors of [30], it may result in a deficiency of the pump energy for inducing cavitation in the beam waist. We verified that supposition by using a thin cell $3a$; its size along the beam amounts to 20 μm, i.e., much less than the beam waist length, so that the SBS process cannot develop inside a cell of such small size. Nonetheless, the pattern of interaction of light waves inside the thin cell, corresponding to Eq. (3), was realized for the broadband pump inside that cell quite similarly to the case of the 20-cm cell, as described further below. Similar to the case of the 20-cm cell, we could not induce cavitation in the 20-μm cell for the narrowband pump even on increasing its intensity by an order of magnitude. Cavitation in the 20-μm cell for degassed water was not explored, because we could not create the hermeticity conditions for that cell.

We have also employed the thin cell for an accurate measurement of the value of the pump intensity at which the bubbles arise. Hereafter, we will denote that value as I'_{thr} to distinguish it from the I_{thr} specified earlier. This is because I_{thr} cannot be considered as a realistic threshold for cavitation. Indeed, measurement of the intensity at which cavitation arises in the 20-cm cell (i.e., I_{thr}) seems likely to be ambiguous because the bubbles appear there along the whole beam waist of length ~0.5 cm, and the beam intensity may alter drastically along that length. At the same time, the pump intensity at which the first bubbles appear in the 20-μm cell can be defined easily in the following way. That cell, placed prior to the focal region, was moved towards the focus until cavitation occurred; the magnitude of intensity was found by dividing the laser beam power (measured in W) by the cross section of beam in the plane of the cell. Additionally, for the thin cell we can oversee and monitor the process of cavitation by taking photographs of bubbles arising in the liquid. This was implemented with the aid of a fluorescent screen 4 (a sheet of paper, which fluoresces on irradiation by uv light), which was placed 2 m behind the cell, along the beam. The process of bubble formation could be projected onto the screen during a laser pulse. The moment at which the intensity I'_{thr} was attained was determined by an appearance on the screen of the characteristic pattern illustrated in Fig. 4. The exposure time of that snapshot was just the laser pulse duration, which means that the bubbles manage to form within a time $\leqslant$20 ns.

Yet again, the size of the bubbles arising was about the spacing between the windows of the cell (20 μm); therefore, they adhered to the windows and did not disappear within a time as long as desired (note that the hydrophilic properties have been specially imparted to the windows, and possible contribution of hydrophobic microinclusions was minimized). The bubbles, therefore, could easily be investigated

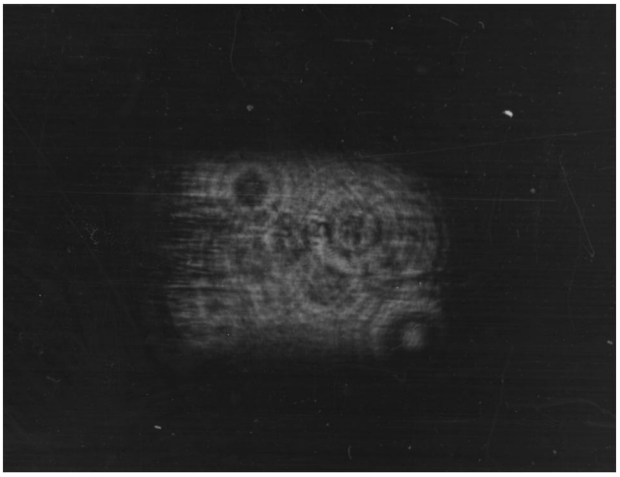

FIG. 4. A formation of the cavitation bubbles in the 20-μm cell.

by an optical microscope, a matter of great convenience. So we can state that the bubbles are quasistable. (Recall that during $\sim$1 s, we observed the track of bubbles floating toward the liquid surface.) The radius R of the bubbles, according to the optical microscope measurements in the thin cell, was 5–10 μm. Knowing the radius R, we can estimate the time T_c for a collapse of these bubbles. To solve this question we should know (apart from the bubble size) the magnitude of pressure at the bubble surface.

While calculating the pressure at the surface of a bubble of such size, we can ignore the term allowing for the surface tension (this term is $\sim$0.1 atm for water). Thus following the study [31], we have $T_c = 0.915R[\rho/(p_{\text{ext}} - p_{\text{in}})]^{1/2}$. Here, ρ is the liquid density, p_{ext} is external pressure, $p_{\text{ext}} \sim p_{\text{atm}}$, where p_{atm} is atmospheric pressure, while p_{in} is the pressure inside the bubble, $p_{\text{in}} = p_g + p_v$, where p_g is the gas pressure and p_v is the vapor pressure. Assuming $p_{\text{in}} \ll p_{\text{ext}}$ (i.e., the vapor-gas mixture is absent inside the bubble), we obtain for the bubbles of size 10 μm an estimate $T_c \sim 1$ μs, which is evidently incongruous to our case. Let us then suppose that the bubbles are purely vaporous, i.e., the cavitation is caused by local laser heating due to the ''hot point'' in the transversal distribution of the beam intensity (see below), and $p_v \sim p_{\text{atm}}$. However, as was shown earlier, the average heating in the caustic is 25 K, i.e., the floating bubble should dissolve even inside the caustic. Indeed, as was indicated for a particular case of a flat liquid-vapor interface, the vapor condensation occurs instantly if the supersaturation coefficient $k = p_v/p_\infty \geqslant 6$ (here p_∞ is the equilibrium vapor pressure; see [32]). In our case ($T = 325$ K and $p_\infty = 0.1$ atm) we find $k = 10$ at $p_v = 1$ atm. This is why we should suggest that the bubbles contain an air-vapor mixture—only in this case does the condition $p_g + p_v \sim p_{\text{atm}}$ become possible.

In concluding this experimental report, we present in Table I the values of I'_{thr} and $Y = (\rho \partial \varepsilon / \partial \rho)$, which is the main material parameter responsible for the generation of hypersound [see Eq. (3)]. These are given for a series of test liquids. [As indicated below, the interaction of light waves of a type corresponding to Eq. (3) takes place in the 20-μm cell for the broadband pump. Hence application of that formula is justified.]

It is clear from Table I that I'_{thr} is less for liquids in which the SBS process proceeds more efficiently. This fact, together with the simultaneous character of the cavitation arising and the Stokes wave in 20-cm cell, reinforces our hypothesis and supposition on the hypersonic nature of cavitation. In what follows, we give a theoretical analysis of the interaction of the hypersonic and optical waves in the field of a broadband laser pump. We also consider possible cavitation mechanisms, which are not due to hypersound.

TABLE I. Values of Y and I'_{thr} for several liquids.

Liquid	Y	I'_{thr} (MW/cm^2)
Hexane	1.07	25.1
Methanol	0.91	26.7
Water	0.87	52.13

III. DISCUSSION

The theory of SBS has been developed in considerable detail elsewhere, including the effect of finite pump bandwidth Δ_+ [33]. Clearly, the characteristics of the process are decisively dependent on the relative magnitudes of Δ_+ and $\Delta_r, \Omega_0, \omega_p$, where $\Delta_r = \Gamma q^2$ is the inverse time of the hypersound damping, $\Gamma = (\xi + 4/3\eta)/\rho$ (the parameters ξ and η were specified above), while $q = \Omega_0/v$ is the hypersonic wave vector ($\Delta_r \sim 10^{-2}$ cm^{-1} in our case); other parameters were specified above. In the transition from virtually monochromatic ($\Delta_+ < \Delta_r$) to more broadband ($\Omega_0 > \Delta_+ > \Delta_r$) pumping, the SBS efficiency decreases in general. However, some special features show up. For instance, a mean-energy threshold is associated with a steep growth of the Stokes wave intensity. On the other hand, the scattering wave pattern does not change. The pump excites the oppositely directed Stokes wave and the copropagating hypersonic wave (see [25]).

With further increase in Δ_+, i.e., when $\Delta_0 < \Delta_+$, the wave pattern of the interaction should become more complicated. Indeed, in the case of the 20-cm cell we can imagine a two-stage process. In the first stage, each spectral component ω_1 of the pump induces an oppositely directed Stokes wave at frequency $\omega_2 = \omega_1 - \Omega_0$ due to SBS. (It was shown in [34] that the Stokes signal spectrum in a field of the broadband pump on the whole is just redshifted by the frequency Ω_0 with respect to the pump spectrum, while the shape of the Stokes signal spectrum remains similar to that of the pump spectrum.) In the second stage, various spectral components of the pump interact with the oppositely directed spectral components of the Stokes signal, thus giving rise to an electrostrictive force at frequency Ω. This is now not necessarily equal to Ω_0. That process is described by a formula analogous to Eq. (3): $p(\Omega = \omega_1 - \omega_2) = (1/8\pi)(\rho \partial \varepsilon / \partial \rho) E_1(\omega_1) E_2^*(\omega_2)$, where $E_{1,2}(\omega_1)$ are the strengths of the electrical field from the spectra of the pump and the Stokes wave, respectively. It is important here that $\omega_{1,2}$ are no longer fixed frequencies. This is in contrast to the case of Eq. (3). Specifically, the frequency ω_1 now sweeps an interval $[\omega_p - \Delta_+/2, \omega_p + \Delta_+/2]$, while the frequency ω_2 sweeps an interval $[\omega_p - \Omega_0 - \Delta_+/2, \omega_p - \Omega_0 + \Delta_+/2]$. That is, the hypersonic frequency range $|\omega_1 - \omega_2|$ is now defined

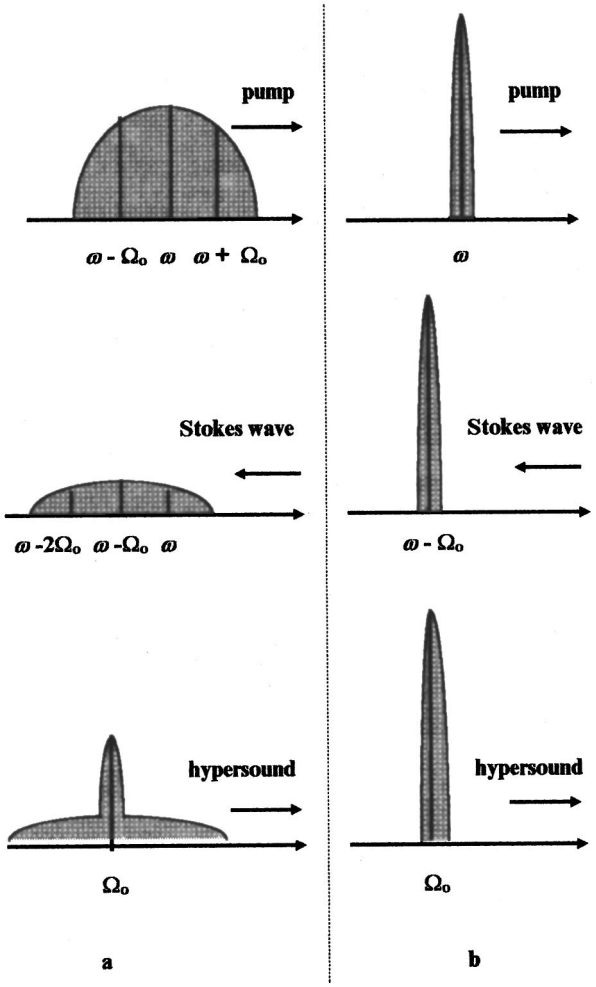

FIG. 5. A schematic of spectral patterns for the pump, the Stokes signal, and the hypersonic wave. (a) A broadband pump case; (b) a narrowband pump case.

by the bandwidth $\sim\Delta_+$. A similar process occurs in the 20-μm cell. Although the process of SBS is evidently absent for such a thin layer of liquid, the beating of frequency-shifted waves takes place owing to overlapping of the wave $E_1(\omega_1)$, taken from the pump spectrum, and the oppositely directed wave $E_2(\omega_2)$, which is also taken from the pump spectrum. The latter wave reflects from the rear window of the cell.

Note, however, that the hypersonic wave at an arbitrary frequency is not necessary amplified in the process described. Indeed, as follows from a simultaneous solution of the equation for the electrostrictive force and the Navier-Stokes equation (see [25,28]), the maximum growth rate is achieved only for a hypersonic wave for which the condition $\Omega_0=\omega_1-\omega_2=(2vn\omega_1/c)$ is satisfied. Therefore, in the case of a broadband pump, the spectrum of the hypersonic wave seems likely to have a high-intensity narrow peak at frequency Ω_0 and low-intensity wings of bandwidth Δ_+. Again, in the case of a narrowband pump, the hypersonic wave spectrum consists only of high-intensity peak at frequency Ω_0. No additional broadband spectral wings are expected here. The schematics of the spectral patterns of the pump, the Stokes signal, and the hypersonic wave for the broadband and narrowband cases are illustrated in Figs. 5(a) and 5(b).

For the broadband pump, it is easy to evaluate an intensity for the hypersonic wave at frequency Ω_0 [i.e., the height of a peak in Fig. 5(a)] for water: $\mathcal{I}\approx 10^{-4}-10^{-2}$ MW/cm^2. The spread in this estimate is associated with the possibility of varying the conditions of pump beam focusing (the length and the radius of the waist) or the angle for pump reflection in the 20-μm cell. At the same time, the intensity of hypersound generated in the experiment with the narrowband pump is $\mathcal{I}_m\approx 10^{-1}-1$ MW/cm^2. This is considerably higher than that in the broadband case.

No previous experimental data on acoustic cavitation thresholds in the hypersonic range are known to us. An extrapolation of the acoustic cavitation threshold $\mathcal{I}_c$ (the latter demonstrates nearly quadratic frequency growth) from the ultrasonic frequency range 10^5-10^6 Hz to the hypersonic frequency range 10^{10} Hz gives $\mathcal{I}_c>100$ MW/cm^2 (for the ultrasonic range, following [1], we can take $\mathcal{I}_c=1$ W/cm^2). This value exceeds an intensity $\mathcal{I}_m\approx 10^{-1}-1$ MW/cm^2 of hypersound generated in the experiment with a narrowband pump, and is much higher than the hypersonic intensity $\mathcal{I}$ in the case of the broadband pump.

A judicious reconciliation of this seemingly experimental paradox can be made by postulating that in the case of broadband pumping, the cavitation is due to resonant excitation of nanobubbles of certain fixed radius R. Indeed, the frequencies about 10^{10} Hz evidently fall into the broad (but low-intensity) spectral wings of hypersound generated in a case of the broadband pump. Assuming that these frequencies are resonances of radial vibrations of nanobubbles, we get from the formula (1) that the nanobubble radius R is about 10 nm. Note that in a resonant situation, high intensities of acoustic waves are presumably not required; they should be just of nonzeroth value, because the efficiency of nanobubble excitation is most likely dictated by the quality of its oscillations; the magnitude of this quality remains unknown for nanobubbles. This interpretation is attractive for us (we leave aside the question of the origin of these nanobubbles and their stabilization) because this is reinforced by the four-photon spectroscopy experiments as well as by a correlation of the cavitation threshold with the efficiency of hypersound stimulation due to the SBS phenomenon. The steady existence of nanobubbles of size 1–10 nm in a settled liquid is associated with the presence of dissolved gas (which has never previously been considered seriously) and suggests a certain mechanism for their stabilization. The model of stable (or long-life) nanobubbles, to which we would welcome challenge, seems intriguing, and if correct evidently has far-reaching consequences.

However, the above interpretation is certainly not the only one; in what follows, we present possible alternative mechanisms for the bubbles formation. Actually, it was shown that the linear absorption of light cannot result in the cavitation. Nonetheless, the bubbles can appear as an effect of laser heating due to the nonlinear phenomena, induced by high-intensity spikes in the laser pulse profile. Indeed, in the case of a broadband pump, we deal with a wide spectrum of longitudinal modes which are able to interfere randomly with one another, giving rise to gigantic ultrashort (of the duration $\propto 1/\Delta\omega_1\sim 10^{-12}$ s) splashes of the light intensity. We can neither confirm nor reject the existence of these splashes,

because they are not resolved by an oscilloscope. We also cannot estimate the real light energy of a particular splash. However, we have some doubts about a dominating role of such splashes in inducing the cavitation. Namely, as the appearance of such a splash has a probabilistic character, the cavitation should be irregular, and the cavitation threshold should have an essential scatter. (In contrast, the formation of bubbles was observed in each pulse if the light intensity was beyond a certain magnitude coinciding with the SBS threshold.) Let us examine, however, a hypothesis of thermal cavitation in a field of a high-intensity laser mode.

It is reasonable to suggest that this hypothesized mode can induce the cavitation by means of its self-focusing and/or an optical breakdown. Starting with the self-focusing analysis, note that in accordance with the study [35], the threshold powers P_s required for this phenomenon at the wavelengths of 1.06 and 0.53 μm are equal to 2.34 and 0.63 MW, respectively. Inasmuch as $P_s = c\lambda^2/32\pi^2 n_2 \propto \lambda^2$, where n_2 is the nonlinear refractive index, we have for the wavelength $\lambda = 308$ nm an estimate $P_s = 0.63(308/532)^2 \approx 2.34(308/1064)^2 \approx 0.2$ MW. However, the optical power of this level (and even higher) is realized both at the broadband ($P = 2.5$ MW) and at the narrowband ($P = 0.5$ MW) pump. As the bubbles formation is absent at the narrowband pump, it seems likely that the cavitation (in our case) cannot be induced by self-focusing.

The model of bubbles formation as a result of an optical breakdown (an optical breakdown is conventionally assumed as the plasma flash in a field of a high-intensity laser field) seems more realistic than the previous mechanism. Note that certain experimental observations do not support the breakdown mechanism, while others are in favor of this mechanism. First of all, we were able to stimulate an optical breakdown (a spark) at tight focusing of both broadband and narrowband Xe-Cl lasing, and also at tight focusing of the third harmonic of YAG:Nd laser radiation (the latter has a wavelength of 350 nm, which is close to the Xe-Cl laser wavelength; the third-harmonic bandwidth was of 0.01 cm^{-1}). The light intensities $\geqslant 10^{11}$ W/cm^2 are required for stimulating a breakdown in water for these wavelengths; this is three orders of magnitude higher than the intensity threshold for the cavitation in water, i.e., the cavitation happens at substantially lower intensities at the broadband pump. (Note that we performed the breakdown experiments in the 20-cm cell, though not in the 20-μm cell, to avoid destroying the windows and littering water by the ablation products.)

It is widely known that the breakdown of liquid is accompanied by the formation of vapor bubbles due to huge plasma temperature (see, for example, [36], where the dynamics of a cavitation bubble resulting from an optical breakdown has been reported). We observed of course the formation of bubbles in the breakdown experiments at the narrowband irradiation, but the behavior of those bubbles was noticeably different from that observed at the low-intensity broadband radiation. Specifically, in the broadband case we saw a continuous track of tiny bubbles which appeared along the whole caustic length and then floated slowly toward the liquid surface (they were seemingly driven by the buoyancy force). In the case of optical breakdown, by contrast, we observed a spark which was followed by an appearance of few relatively large bubbles. These bubbles immediately flew out of the breakdown area; they were driven by hydrodynamic fluxes, so they did not necessarily move strictly upward. Thus we should conclude that if the low-threshold cavitation regime is indeed due to an optical breakdown at the broadband irradiation of a liquid, this breakdown has too extravagant features. First of all, it appears only at the broadband irradiation, and second, it is free of plasma spark (the main manifestation of breakdown).

However, there exist certain arguments in favor of the breakdown mechanism as the possible reason for the broadband cavitation. Indeed, let us assume that the hypothesized ultrashort intensity splashes (see above) have an intensity of $\sim 10^{11}$ W/cm^2, which is sufficient to induce an optical breakdown. These high-intensity splashes can be realized as the modes of a very small cross section, i.e., a transversal structure of the beam is highly inhomogeneous and has the ''hot points.'' To determine a contribution of these ''hot points,'' we placed two Iris diaphragms inside the laser cavity on each side of an active element, and the laser beam cross section was cut down to 1 mm (actually to the level of breaking the laser generation). However, if the pulse energy was kept on a steady level (this was achieved by an amplifier), the effect did not vanish at the broadband pump. Furthermore, an expansion of diaphragms did not lead to the cavitation arising at the narrowband pump (provided that the plasma spark was absent).

These observations, however, do not dismiss the possibility of the existence of these high-intense modes—they can appear very close to the cavity axis and have a too small cross section to be cut by a diaphragm. Thus we cannot discard completely an optical breakdown by a random high-intensity mode as the reason for the formation of bubbles. Besides, the threshold of liquid breakdown (say, by a YAG:Nd laser in water) grows significantly after degassing (see [21–23]), which also supports this alternative mechanism. However, the bubble formation mechanism at such short-time splashes is unclear. (Indeed, we have demonstrated that the bubbles manage to be formed during the laser pulse, and if the process is due to the ultrashort splashes, we could assume the bubbles formation is completed during such a splash, i.e., within 10^{-12} s.) Moreover, this mechanism assumes that the formation of bubbles is due to heating, and the bubbles should be purely vaporous. However, as follows from above, the vaporous bubbles can hardly be realized in our case. And finally, if the phenomenon observed is a specific manifestation of optical breakdown at the broadband uv pump, then the data on the four-photon spectroscopy from degassed and nondegassed water have no relation to the bubbles formation, and the correlation between the efficiency of hypersound generation and inducing the cavitation is just a curious but inexplicable fact.

Summarizing, the hypothesis about the resonant hypersonic cavitation can be confirmed (or rejected) in experiment on inducing an intense hypersound at a variable frequency (the tuning of the pump frequency over a rather wide uv range is required for this).

ACKNOWLEDGMENT

This research was supported by the Russian Foundation for Basic Research (Project Code Nos. 98-02-16264 and 99-15-96023).

[1] M. G. Sirotyuk, *Experimental Investigations of Ultrasonic Cavitation*, in *High Intensity Ultrasonic Fields*, edited by L. D. Rozenberg (Plenum, New York, 1971).
[2] P. S. Epstein and M. S. Plesset, J. Chem. Phys. **18**, 1505 (1950).
[3] V. A. Akulichev, Zh. Akust. **12**, 160 (1997) [Sov. Phys. Acoust. **12**, 144 (1966)].
[4] F. E. Fox and K. F. Herzfeld, J. Opt. Soc. Am. **26**, 985 (1954).
[5] K. F. Herzfeld, in *Proceedings of the First Symposium on Naval Hydrodynamics*, edited by F. S. Sherman (National Academy of Science, Washington, DC, 1957), p. 319.
[6] M. Strasberg, J. Opt. Soc. Am. **31**, 163 (1959).
[7] M. G. Sirotyuk, Zh. Akust. **16**, 286 (1970) [Sov. Phys. Acoust. **16**, 237 (1970)].
[8] M. G. Sirotyuk, Zh. Akust. **16**, 567 (1971) [Sov. Phys. Acoust. **16**, 482 (1971)].
[9] D. E. Yount, T. D. Hunkle, J. S. D'Arrigo, F. W. Ingle, C. M. Yeung, and E. L. Beckman, Aviat., Space Environ. Med. **48**, 185 (1977).
[10] D. E. Yount, J. Opt. Soc. Am. **65**, 1429 (1978).
[11] E. N. Harvey, K. K. Barnes, W. D. McElroy, A. H. Whitely, D. C. Pease, and K. W. Cooper, J. Cell. Comp. Physiol. **24**, 1 (1944).
[12] R. E. Apfel, J. Opt. Soc. Am. **48**, 1179 (1970).
[13] R. H. S. Winterton, J. Phys. D **10**, 2041 (1977).
[14] L. A. Crum, Nature (London) **278**, 148 (1979).
[15] L. A. Crum, in *Cavitation and Inhomogeneities in Underwater Acoustics*. edited by W. Lauterborn (Springer-Verlag, New York, 1980).
[16] M. Minnaert, Philos. Mag. **16**, 7 (1933); **16**, 235 (1933).
[17] N. F. Bunkin, A. I. Kuklin, A. V. Lobeyev, T. G. Movchan, and O. I. Vinogradova, Pis'ma Zh. Eksp. Teor. Fiz. **62**, 688 (1995) [JETP Lett. **62**, 685 (1995)].
[18] V. P. Skripov, *Metastable Liquids* (Wiley, Chichester, 1974), Israel Progr. Sci. Transl.
[19] B. E. Noltingk and E. A. Neppiras, Proc. Phys. Soc. London, Sect. B **63**, 674 (1950).
[20] R. Macleay and L. Holroyd, J. Appl. Phys. **32**, 449 (1961).
[21] W. P. Roach, M. E. Rogers, B. A. Rockwell, S. A. Boppart, C. D. Stein, and C. M. Bramlette, Aviat., Space Environ. Med. **65**(5, Suppl.), A100 (1994).
[22] N. F. Bunkin and A. V. Lobeyev, Phys. Lett. A **229**, 327 (1997).
[23] N. F. Bunkin, O. A. Kiseleva, A. V. Lobeyev, T. G. Movchan, B. W. Ninham, and O. I. Vinogradova, Langmuir **13**, 3024 (1997).
[24] I. L. Fabelinskii, *Molecular Scattering of Light* (Plenum, New York, 1981).
[25] Y. R. Shen, *The Principles of Nonlinear Optics* (Wiley, New York, 1984).
[26] N. F. Bunkin, A. F. Bunkin, A. V. Lobeyev, and A. A. Nurmatov, Phys. Lett. A **225**, 349 (1997).
[27] R. Battino, M. Banzhof, M. Bogan, and E. Wilhelm, Anal. Chem. **43**, 806 (1971).
[28] L. D. Landau and E. M. Lifshitz, *Electrodynamics of Continuous Media* (Pergamon, Oxford, 1984).
[29] V. B. Karpov, V. V. Korobkin, and D. A. Dolgolenko, Phys. Lett. A **158**, 350 (1991).
[30] E. Armandillo and D. Proch, Opt. Lett. **8**, 523 (1983).
[31] J. W. Rayleigh, Philos. Mag. **34**, 94 (1917).
[32] J. Frenkel, *Kinetic Theory of Liquids* (Dover, New York, 1955).
[33] B. Ya. Zel'dovich, N. F. Pilipetskii, and V. V. Shkunov, *Principles of Phase Conjugation* (Springer, New York, 1985).
[34] N. F. Bunkin, G. A. Lyakhov, and O. V. Umnova, Zh. Eksp. Teor. Fiz. **104**, 3287 (1993) [Sov. Phys. JETP **77**, 549 (1993)].
[35] W. L. Smith, P. Liu, and N. Bloembergen, Phys. Rev. A **15**, 2396 (1977).
[36] A. Vogel, W. Hentshel, J. Holzfuss, and W. Lauterborn, Opthalmology (Philadelphia) **93**, 1259 (1986).